

# Concept and Systematic Investigation of the Bunch-to-Bucket Transfer between the FAIR Accelerators

J. Bai<sup>1,2\*</sup> and T. Ferrand<sup>1,3</sup>, O. Kester<sup>4</sup>, D. Ondreka<sup>1</sup>, D. Beck<sup>1</sup>, C. Prados<sup>1,3</sup>

1. GSI Helmholtzzentrum für Schwerionenforschung, 64291 Darmstadt, Germany

2. IAP, Goethe-Universität, Frankfurt am Main, 60439 Frankfurt am Main, Germany

3. TEMF, Technische Universität Darmstadt, 64291 Darmstadt, Germany

4. TRIUMF, 4004 Wesbrook Mall Vancouver, BC V6T 2A3 Canada

The Facility for Antiproton and Ion Research (FAIR) project is aiming at providing high-energy beams of ions of all elements from hydrogen to uranium, as well as antiprotons and rare isotopes with high intensities. The existing accelerator facility of GSI Helmholtz center for Heavy Ion Research GmbH (short: GSI) and the future FAIR facility employ a variety of circular accelerators like heavy ion synchrotrons (the SIS18 and the SIS100) and storage rings (the experimental storage ring ESR, the CRYRING@ESR (short: CRYRING), the collector ring CR and the high energy storage ring HESR) for the preparation of secondary beams and experiments. Bunches are required to be transferred into rf buckets among GSI and FAIR circular accelerators for different purposes. All this imposes new requirements on the bunch-to-bucket transfer system. In order to fulfill all requirements, a completely new and unique FAIR bunch-to-bucket transfer system will be developed. The presentation of the concept of the system and the systematic investigation from timing perspective are the purpose of this paper. The concept and basic procedure of the system first of all are presented. Afterwards, a systematic investigation from the beam dynamics and timing requirement of the transfer is analyzed. Finally, the application of the system for all FAIR use cases is summarized.

**PACS numbers:** 29.20.D-; 29.27.Ac; 07.05.Dz

## I. INTRODUCTION

FAIR is a new international accelerator facility under construction at GSI. It is aiming at providing high-energy beams of ions of all elements from hydrogen to uranium with high intensities, as well as beams of rare isotopes and of antiprotons [1, 2]. The FAIR facility in its start version will consist of three circular accelerators (short: ring), the SIS100, the CR and the HESR. In addition, the GSI accelerator facility complements the planned accelerators of FAIR, which comprises the SIS18, the ESR and the CRYRING. Bunches are required to be transferred into radio frequency (rf) buckets among GSI and FAIR rings by the so-called bunch-to-bucket (B2B) transfer method. An implementation of the B2B transfer from the SIS18 to the ESR exists, the phase difference between the two rf systems is measured based on the direct transmission of the analog rf signals of the two rings to a central station. However the direct transmission is undesired for the new FAIR accelerator complex, which will be around six times larger than the existing GSI site. In order to avoid the direct transmission, a center clock can be used, which provides a reference clock to the rf systems of the two rings. The phase difference between the rf system and the reference clock is measured at each ring locally and the measurement results are transferred to a central station to calculate the phase difference. Coincidentally, the FAIR Bunchphase Timing System (BuTiS) [3] can provide such a reference clock for the B2B transfer, which serves as a campus-wide clocks distribution system for

the low level radio frequency (LLRF) system [4] with sub nanosecond resolution and stability over distances of several hundred meters [5]. In addition, the FAIR new timing system, the General Machine Timing (GMT) system [6], is based on the sub-nanosecond synchronization White Rabbit (WR) network [7], which can transfer the measurement results deterministically. Therefore, a new FAIR B2B transfer system based on the GMT system, the LLRF system and the BuTiS is required.

The concept of the B2B transfer was first introduced in the early 1980s at the European Organization for Nuclear Research (CERN) for the beam transfer from the Proton Synchrotron Booster (PSB) to the PS [8] and the B2B transfer has been used for almost three decades around the world. The FAIR B2B transfer is comparable with the CERN B2B transfer. At CERN, primary beams of ions of all elements can be transferred among rings as at FAIR, e.g. the Large Hadron Collider (LHC) is supplied with 7 TeV high energy proton beams from the injector chain PSB - Proton Synchrotron (PS) - Super Proton Synchrotron (SPS) and with 2.76 TeV/u high energy heavy ion beams from the injection chain Low Energy Ion Ring (LEIR) - PS - SPS [9]. In addition, the CERN B2B transfer system transfers the secondary beams to rf buckets, e.g. a proton beam that comes from the PS is fired into an antiproton (pbar) target to produce the antiproton beam and the antiproton beam is transferred into Antiproton Decelerator (AD). However, the CERN B2B transfer is based on the direct transmission of the analog signal (e.g. the revolution frequency signal of the target ring) from the target ring to the source ring as the GSI existing B2B transfer implementation, which is used for the bucket counting and synchronization. The instability of every analog signal transmission delay along

---

\* Email: baijiaoni1314@gmail.com

coaxial cables or optical fibers (e.g. the thermal drift) is compensated individually. In order to synchronize two rings, the beam of the source ring is moved to an off-momentum position by adjusting the cavities frequency (the magnetic field is constant). A periodic beating of the phase between the revolution signals of the two rings is observed. The relative azimuthal position between the two rings is measured and the beam is moved back to the reference momentum when it reaches the correct azimuth [10]. The synchronization process between the PS and the SPS takes about 50 ms [11] and that between the SPS and the LHC takes about 30 ms [12].

The FAIR B2B transfer system avoids the direct analog signal transmission. It makes use of not only the mentioned azimuthal position correction as CERN to realize the synchronization process, but also the automatically azimuthal position correction with the help of the circumference ratio between two rings, which decreases the time duration of the synchronization process.

In the following section, the requirements for the FAIR B2B transfer system is listed. In Sec. III the concept of the FAIR B2B transfer system is introduced together with the basic procedure. The FAIR B2B transfer system focus first of all on the transfer from the SIS18 to the SIS100. Hence, the Sec. IV is concerned with the analysis of the two synchronization methods from the beam dynamics for the B2B transfer from the SIS18 to the SIS100. In Sec. V, the timing constraints of the system is presented. Afterwards the application of the system for FAIR use cases is presented in Sec. VI.

## II. REQUIREMENTS FOR THE FAIR B2B TRANSFER SYSTEM

The FAIR B2B transfer system should support primary beam transfers with a tolerable bunch-to-bucket injection center mismatch ( $\pm 1^\circ$  for most FAIR use cases) and within an upper bound time (10 ms for most FAIR use cases), e.g. bunches are transferred from the SIS18 to the SIS100, from the SIS18 to the ESR and further to the CRYRING, from the CR to the HESR. It must be flexible to support the beam transfer between two rings with an arbitrary ratio in their circumferences, e.g. the circumference ratio between the SIS100 and the SIS18 is 5, an integer, between the SIS18 and the ESR is  $2 - 0.003$ , close to an integer and between the HESR and the CR is  $2.6 - 0.003$ , far away from an integer.

The difficulty is to transfer beams separated by fragmentation into the target ring with a tolerable bunch-to-bucket injection center mismatch (e.g.  $\pm 10^\circ$  mismatch for the ESR barrier bucket injection), because secondary beams have arbitrary energy compared with primary beams. For example, one 28.8 GeV/u proton bunch extracted from the SIS100 is transferred to the pbar target, producing a 3 GeV/u antiproton bunch. Further the antiproton bunch is injected into a CR bucket. One 550 MeV/u heavy ion bunch extracted from the SIS18

is transferred to a target and a 400 MeV/u rare isotope beam (RIB) bunch is separated by the fragment separator (FRS) and further transferred into an ESR bucket. One 1.5 GeV/u heavy ion bunch extracted from the SIS100 is transferred to a target and a 740 MeV/u RIB bunch is separated by a superconducting FRS (Super-FRS) and further transferred into a CR bucket.

Several B2B transfers running at the same time are required, e.g. the B2B transfer from the SIS18 to the SIS100 and at the same time the B2B transfer from the ESR to the CRYRING. It should be capable to transfer beam of different ion species from one machine cycle to another. Various complex bucket filling patterns should be supported, e.g. eight out of ten SIS100 buckets are filled by four SIS18 batches, each of two bunches. In addition, it should coordinate with the machine protection system, which protects the SIS100 and subsequent accelerators or experiments from beam induced damage. The beam transfer must be indicated for the beam instrumentation.

## III. CONCEPT OF THE FAIR B2B TRANSFER SYSTEM

The new FAIR B2B transfer system relies on the FAIR GMT system, the LLRF system and the BuTiS. The GMT system synchronizes all Front End Controllers (FEC) with nanosecond accuracy over the whole FAIR campus and distributes timing messages to all FECs via the reliable and robust WR network and controls all FECs to execute real-time actions at a designated time [13]. The GMT system mainly consists of a data master (DM), the WR network and FECs. The DM defines the accelerator schedule. The Scalable Control Unit (SCU) [14] is a new generation of the standard FEC for the FAIR control system, which provides a compact and flexible solution for controlling all types of accelerator equipment. The LLRF system synchronizes cavities in every ring by means of a reference rf signal distribution system (short: rf system) [15]. The BuTiS can provide campus-wide reference clock signals with same frequency and in phase.

In order to complete the B2B transfer, first of all, the rf systems of the source and target rings must be correctly aligned in phase. Secondly, the trigger for the extraction and injection kicker magnets must be synchronized with the beam. Finally the time point of the actual beam injection into the target ring must be indicated to enable beam instrumentation devices to measure the properties and the behavior of the beam directly after the injection. In the following, the realization of these three functionalities will be presented. For the B2B transfer, a so-called B2B transfer master is defined, which is responsible for the data collection of two rings, the data calculation, the data redistribution and the B2B transfer status check. For the sake of simplicity, a specific SCU located at the source ring fulfills this function, see III C.

### A. Phase Alignment

In order to realize the phase alignment, the phase difference  $\Delta\phi$  between the two rf systems of the two rings must be obtained. The phase difference is indirectly measured via a FAIR campus wide distributed reference signal synchronized with BuTiS clocks.

$$\begin{aligned}\Delta\phi &= (\Delta\phi_1 - \Delta\phi_2) \mod 2\pi \\ &= [2\pi(f_1 - f_{ref})t + \phi_1] \\ &\quad - [2\pi(f_2 - f_{ref})t + \phi_2] \mod 2\pi \\ &= [2\pi(f_1 - f_2)t + \phi_1 - \phi_2] \mod 2\pi\end{aligned}\quad (1)$$

where  $\phi_1$  and  $\phi_2$  are the initial phases of the two rf systems of the source and target rings,  $f_1$  and  $f_2$  the frequencies of the two rf systems,  $f_{ref}$  the frequency of the reference signal and  $\Delta\phi_1$  and  $\Delta\phi_2$  the phase difference between the two rf systems and the reference signal.

For the phase difference, there are two scenarios according to the relation between  $f_1$  and  $f_2$ . When  $f_1$  equals to  $f_2$ ,  $\Delta\phi$  is constant. In order to change the phase difference for the phase alignment, the phase of either (or both) rf system must be shifted by modulating the frequency of the rf system away from the reference value for a specific period of time and then modulating back. This is called “phase shift”.

When  $f_1$  and  $f_2$  are slightly different,  $\Delta\phi$  is a periodic linear function whose rate is the difference between the two frequencies. This is called “frequency beating”. The periodically variable rate is called the “beating frequency”,  $\Delta f = |f_1 - f_2|$ . The beating period is defined as a period of time for the periodical variation, namely  $1/\Delta f$ . Within one beating period, there exists a time point, which corresponds to a correct phase difference between the two rf systems, namely the phase alignment.

As a consequence, the phase alignment is realized based on two identical or two slightly different frequencies. These two frequencies are called “synchronization frequencies”, denoted as  $f_{syn}^X$ , where X indicates either the source or target ring (e.g.  $f_{syn}^{src}$  and  $f_{syn}^{trg}$ ). The phase difference between the two synchronization frequencies is denoted as  $\Delta\phi_{syn}$ . The number of circulating buckets is determined by the harmonic number  $h_{rf}^X$  and the cavity rf frequency is the harmonic number times of the revolution frequency, namely  $f_{rf}^X = h_{rf}^X \cdot f_{rev}^X$ , where the cavity rf frequency is denoted as  $f_{rf}^X$  and the revolution frequency  $f_{rev}^X$ . The FAIR LLRF system produces the revolution frequency as the 1<sup>st</sup> harmonic and supports not only the integer multiple but also the fractional multiple of the revolution frequency. For all FAIR use cases, the two synchronization frequencies are an integer multiple of the same or slightly different derived rf frequencies, which are the fraction of the revolution frequencies.

$$f_{syn}^X = Y \cdot f_{rev}^X / m \quad (2)$$

where  $f_{rev}^X/m$  represents the fraction of the revolution frequency and both  $m$  and  $Y$  are positive integers, which

are determined by the circumference ratio and the harmonic numbers.

- For FAIR use cases with an integer ratio in their circumferences, there is the following ratio between two cavity rf frequencies

$$\frac{f_{rf}^l}{f_{rf}^s} = \frac{h_{rf}^l}{h_{rf}^s \cdot \kappa} \quad (3)$$

where  $\kappa$  is the circumference ratio between the large and small rings. The superscript  $l$  and  $s$  represent the large and small rings.

In this case, there exists two identical synchronization frequencies.

$$f_{syn}^l = \frac{f_{rf}^l}{h_{rf}^l/Y} = Y f_{rev}^l \quad (4)$$

$$f_{syn}^s = \frac{f_{rf}^s}{h_{rf}^s \kappa/Y} = \frac{Y}{\kappa} f_{rev}^s \quad (5)$$

$Y$  is the great common divisor (GCD) of  $h_{rf}^l$  and  $h_{rf}^s \cdot \kappa$ .

For example, the  $H^+$  B2B transfer from the SIS18 to the SIS100 with  $\kappa = 5$  and  $Y = 5$  has  $f_{syn}^{SIS100} = 5 f_{rev}^{SIS100}$  and  $f_{syn}^{SIS18} = f_{rev}^{SIS18}$ , see Fig. 1. For detailed parameters of the FAIR B2B transfer from the SIS18 to the SIS100, please see Appendix. B 1.

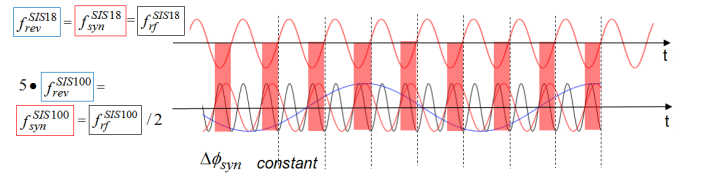


FIG. 1. Example of the synchronization frequencies in the scenario of an integer circumference ratio between two rings.

The example is the FAIR use case of the  $H^+$  B2B transfer from SIS18 to SIS100.

- For FAIR use cases with a close to an integer ratio in their circumference, there is a close to an integer multiple relationship between the two revolution frequencies.

$$\frac{f_{rev}^s}{f_{rev}^l} = \kappa + \lambda \quad (6)$$

where  $\kappa + \lambda$  is the circumference ratio between the large and small rings.  $\kappa$  is an integer and  $|\lambda| \leq 0.005$ .

The ratio between two cavity rf frequencies is

$$\frac{f_{rf}^l}{f_{rf}^s} = \frac{h_{rf}^l}{h_{rf}^s \cdot (\kappa + \lambda)} = \frac{h_{rf}^l}{h_{rf}^s \cdot \kappa + h_{rf}^s \cdot \lambda} \quad (7)$$

Two synchronization frequencies are

$$f_{syn}^l = \frac{f_{rf}^l}{h_{rf}^l/Y} = Y f_{rev}^l \quad (8)$$

$$f_{syn}^s = \frac{f_{rf}^s}{h_{rf}^s \kappa/Y} = \frac{Y}{\kappa} f_{rev}^s \quad (9)$$

$Y$  is the GCD of  $h_{rf}^l$  and  $h_{rf}^s \cdot \kappa$ .

For example, four bunches transfer from the SIS18 to the ESR with  $\kappa + \lambda = 2 - 0.003$  and  $Y = 4$  has  $f_{syn}^{SIS18} = 4 f_{rev}^{SIS18}$  and  $f_{syn}^{ESR} = 2 f_{rev}^{ESR}$ , see Fig. 2. For detailed parameters of the FAIR B2B transfer from the SIS18 to the ESR, please see Appendix. B2.

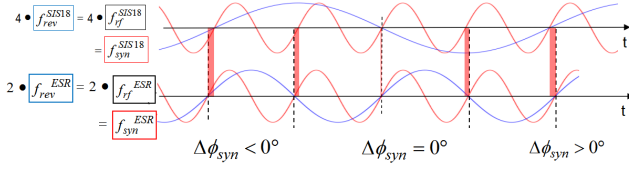


FIG. 2. Example of the synchronization frequencies in the scenario of a close to an integer circumference ratio between two rings.

*The example is the FAIR use case of four bunches transfer from SIS18 to ESR.*

- For quite many FAIR use cases with the ring circumference ratio far away from an integer, the two revolution frequencies are very different and can be expressed as

$$\frac{f_{rev}^s}{f_{rev}^l} = \frac{m}{n} + \lambda \quad (10)$$

where  $m$  and  $n$  are integers and  $|\lambda| \leq 0.05$ .

The ratio between two cavity rf frequencies is

$$\frac{f_{rf}^l}{f_{rf}^s} = \frac{h_{rf}^l \cdot n}{h_{rf}^s \cdot m + h_{rf}^s \cdot \lambda \cdot n} \quad (11)$$

Two synchronization frequencies are

$$f_{syn}^l = \frac{f_{rf}^l}{h_{rf}^l n/Y} = \frac{Y}{n} f_{rev}^l \quad (12)$$

$$f_{syn}^s = \frac{f_{rf}^s}{h_{rf}^s m/Y} = \frac{Y}{m} f_{rev}^s \quad (13)$$

$Y$  is the GCD of  $h_{rf}^l \cdot n$  and  $h_{rf}^s \cdot m$ .

For example, the B2B transfer from the CR to the HESR with  $m/n = 26/10$ ,  $\lambda = 0.003$  and  $Y = 2$

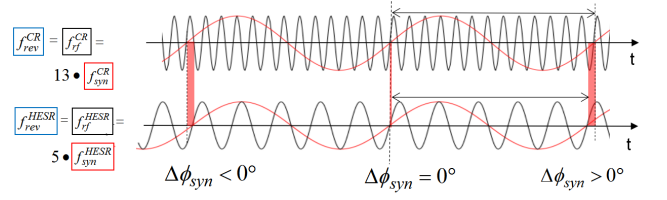


FIG. 3. Example of the synchronization frequencies in the scenario of a far away from an integer circumference ratio between two rings.

*The example is the FAIR use case of the B2B transfer from CR to HESR.*

has  $f_{syn}^{CR} = 2 \cdot f_{rev}^{CR}/26$  and  $f_{syn}^{HESR} = 2 \cdot f_{rev}^{HESR}/10$ , see Fig. 3. For detailed parameters of the FAIR B2B transfer from the CR to the HESR, please see Appendix. B5.

For the 1<sup>st</sup> scenario, the two synchronization methods are available for the phase alignment of the two rf systems, the phase shift method and the frequency beating method. For the 2<sup>nd</sup> and 3<sup>rd</sup> scenarios, only the frequency beating method is available. Both methods provide a time frame for the B2B transfer, within which bunches are transferred into buckets with a certain bunch-to-bucket injection center mismatch smaller than a given upper bound (e.g.  $\pm 1^\circ$ ). This time frame is called the synchronization window.

#### 1. Phase shift method

The required phase shift  $\Delta\phi_{syn}$  depends on the frequency modulation  $\Delta f_{syn}$  and the duration  $T$ .

$$\Delta\phi_{syn} = 2\pi \int_{t_0}^{t_0+T} \Delta f_{syn}(t) dt \quad (14)$$

where  $t_0$  is the start time of the phase shift.

During the phase shift process, beam is moved to off-momentum by adjusting frequency (the magnetic field is constant) and moved back to the reference momentum after the certain duration. After the phase shift, bunches of the source ring are phase aligned with buckets of the target ring. The synchronization window is defined as the time frame after the rf frequency modulation, see Fig. 4.

The phase shift process must be performed slowly enough to preserve the longitudinal emittance. In summary the rf frequency modulation function must meet the following requirements.

- There is a maximum value for  $\Delta f_{rf}$ , which is constrained by the maximum tolerable relative momentum shift  $\Delta p/p$  [16].  $\Delta p/p$  is constrained by the semi-aperture required for the beam and the dispersion function.

$$\frac{\Delta p}{p} = \frac{1}{\frac{1}{\gamma^2} - \alpha_p} \cdot \frac{\Delta f_{rf}}{f_{rf}} \Big|_{\frac{\Delta B}{B}=0} \quad (15)$$

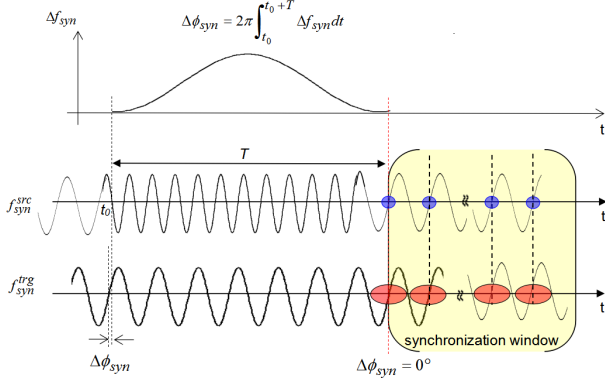


FIG. 4. Example for the phase shift method with a sinusoidal rf frequency modulation.

Blue dots represent bunches of the source ring and red dots buckets of the target ring.

where  $\gamma$  is the relativistic factor, which measures the total particle energy in units of the particle rest energy and  $\alpha_p$  is the momentum compaction factor.

- The 1<sup>st</sup> time derivative of  $\Delta f_{rf}$  must be continuous, so that the synchronous phase changes continuously for the beam to follow.

$$\begin{aligned} V_0 \phi_s &\approx V_0 \sin \phi_s = 2\pi R \rho \dot{B} = \frac{2\pi R B \rho}{p} \frac{d\Delta p}{dt} \\ &= \frac{2\pi R B \rho}{(1/\gamma^2 - \alpha_p) f_{rf}} \frac{d\Delta f_{rf}}{dt} \end{aligned} \quad (16)$$

where  $V_0$  is the amplitude of the rf voltage,  $\phi_s$  the synchronous phase,  $B$  the magnetic field,  $\rho$  the bending radius of a particle immersed in a magnetic field  $B$ ,  $R$  the average orbit radius and  $q$  the charge of a particle.

- The 1<sup>st</sup> time derivative of  $\Delta f_{rf}$  must be small enough to guarantee that the bucket acceptance enables to capture bunches. The ratio of the bucket size of a running bucket to that of a stationary bucket is called the “bucket area factor”, denoted as  $\alpha_b$  [17].

$$\alpha_b(\phi_s) \approx \frac{1 - \phi_s}{1 + \phi_s} \quad (17)$$

The bucket area factor is inversely proportional to the synchronous phase, which is proportional to the 1<sup>st</sup> time derivative of  $\Delta f_{rf}$ .

- The 2<sup>nd</sup> time derivative of  $\Delta f_{rf}$  must be small enough, so that the change rate of the synchronous phase is slow enough for the beam to follow. The 2<sup>nd</sup> time derivative of  $\Delta f_{rf}$  is reflected by the parameter of the adiabaticity  $\varepsilon$  [18].

$$\varepsilon \approx \frac{1}{2\omega_s} |\phi_s \dot{\phi}_s| \quad (18)$$

where  $\omega_s$  is the angular synchrotron frequency.

The adiabaticity  $\varepsilon$  is proportional to  $\dot{\phi}_s$ , which is proportional to the 2<sup>nd</sup> time derivative of  $\Delta f_{rf}$ .

In order to accomplish the phase alignment as fast as possible, the phase shift will be conducted backward and forward for FAIR. Therefore a phase shift of up to  $\pm\pi$  will be considered for rf systems with regard to the synchronization frequency  $f_{syn}^X$ . Besides, a normalized frequency modulation profile  $f_{normalized}$  for  $\pi$  must be precalculated, which meets the requirements mentioned above. The actual frequency modulation profile  $f_{actual}$  is decided by  $f_{normalized}$  and the required phase shift  $\Delta\phi_{syn}$ .

$$f_{actual}(t) = \frac{\Delta\phi_{syn}}{\pi} f_{normalized}(t) \quad (19)$$

## 2. Frequency beating method

The frequency beating method uses two slightly different synchronization frequencies. When the two synchronization frequencies are slightly different, the two rf systems are beating automatically. When they are identical, one (or both) rf system is detuned to achieve the beating. The frequency is detuned at constant energy by changing the radius and the magnetic field ( $\Delta p/p = 0$ ). The frequency detuning is constrained by the relative orbit length change  $\Delta L/L$  [16].

$$\frac{\Delta f_{rf}}{f_{rf}} = -\frac{\Delta L}{L} \quad (20)$$

The synchronization window is defined as a symmetric time frame with respect to the time, when the phase difference between the two synchronization frequencies is closest to the required phase difference, see Fig. 5. The length of the synchronization window  $T_w$  is defined in the later part.

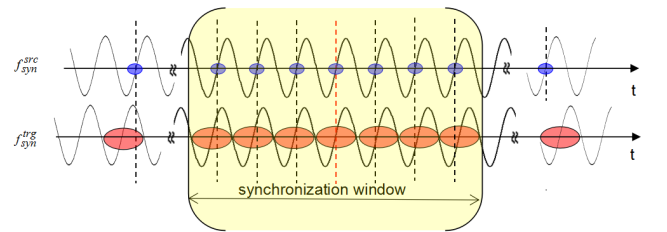


FIG. 5. Illustration of the frequency beating method. Blue dots represent bunches of the source ring and red dots buckets of the target ring.

The bunch-to-bucket injection center mismatch within the synchronization window  $\sigma_{rf}$  is calculated by

$$\sigma_{rf} = \pm \frac{1}{2} \cdot 2\pi |f_{syn}^{src} - f_{syn}^{trg}| \cdot T_w \cdot \frac{f_{rf}^{trg}}{f_{syn}^{trg}} \quad (21)$$



In conclusion, the frequency beating method is preferable for the FAIR project, because it is applicable for the B2B transfer with either an integer or non integer circumference ratio. In addition, it reduces the duration of the B2B transfer process (e.g. 10 ms is an upper bound for most FAIR use cases), because the rf frequency detuning is executed during the rf acceleration ramp. For the phase shift method, the rf frequency modulation must be executed slowly enough at the rf flattop for beams to follow according to the criteria. The phase shift method therefore needs much longer time to be executed. However, there are also some advantages of the phase shift method. The synchronization window is relatively long and the B2B injection center mismatch is approximately  $0^\circ$ . Besides, the duration of the rf frequency modulation is known in advance and the time point for the transfer is predictable. The phase of the rf system can jump to a desired value, when there is no bunch at the ring.

### B. Trigger of Extraction and Injection Kickers

The phase alignment provides a synchronization window, within which bunches can be transferred into buckets with the B2B injection center mismatch smaller than an upper bound (e.g.  $\pm 1^\circ$ ). This process is called “coarse synchronization”. Furthermore, within the synchronization window the extraction kicker must kick bunches exactly the time-of-flight earlier before a specific bucket passes the injection kicker. This process is called “fine synchronization”. The fine synchronization requires the kicker firing based on a bucket indication signal  $f_{bucket}$  for the 1<sup>st</sup> bucket of the target ring plus a fixed delay (e.g. the time-of-flight) [19]. The combination of the two synchronization processes achieves that bunches are injected into correct buckets with required B2B injection center mismatch. Fig. 6 illustrates the two synchronization processes.

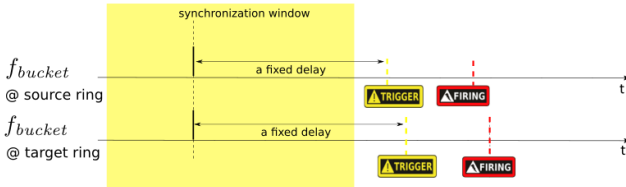


FIG. 6. Coarse and fine synchronization processes.

For FAIR use cases, either  $m/Y$  or  $Y/m$  is an integer for eq. 2. In other words, either the revolution period is an integer multiple of the period of the synchronization frequency or the period of the synchronization frequency is an integer multiple of the revolution period. The bucket indication signal needs to indicate not only the 1<sup>st</sup> bucket of the target ring, but also the starting point of the phase alignment with the rf system of the source ring, therefore the bucket indication signal,

$f_{bucket}$ , has the smaller value of  $f_{rev}^{trg}$  or  $f_{syn}^{trg}$ . For example, the  $H^+$  B2B transfer from the SIS18 to the SIS100 has  $f_{bucket} = f_{rev}^{trg}$  (see Fig. 7) and the B2B transfer from the CR to the HESR has  $f_{bucket} = f_{syn}^{trg}$  (see Fig. 8). The length of the synchronization window is one period of the bucket indication signal.

$$T_w = \frac{1}{f_{bucket}} = \begin{cases} T_{rev}^{trg} & f_{syn}^{trg} \geq f_{rev}^{trg} \\ T_{syn}^{trg} & f_{syn}^{trg} < f_{rev}^{trg} \end{cases} \quad (22)$$

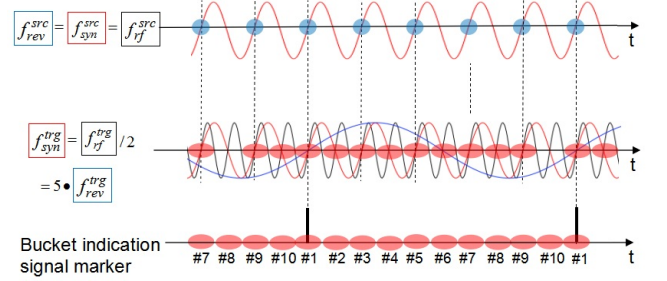


FIG. 7. Frequency of the bucket indication signal equals to the revolution frequency of the target ring.

This example is the FAIR use case of the  $H^+$  B2B transfer from the SIS18 to the SIS100. The correct phase alignment of the two rf systems is assumed with  $\Delta\phi_{syn} = 0^\circ$  and only the buckets with the odd number (e.g. #1, #3) are to be filled in this example.

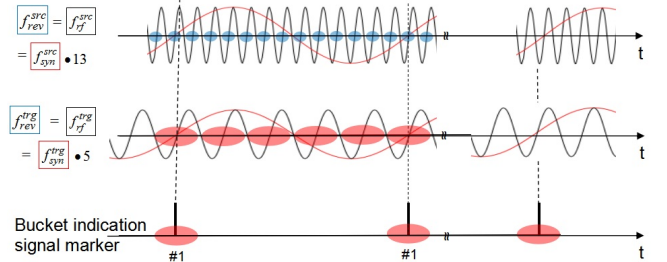


FIG. 8. Frequency of the bucket indication signal equals to the synchronization frequency of the target ring.

This example is the FAIR use case of the B2B transfer from the CR to the HESR.

### C. Beam Indication for Beam Instrumentation Devices

Specific SCUs for the B2B transfer are required, including a B2B source SCU and a source trigger SCU at the source ring and a B2B target SCU and a target trigger SCU at the target ring. The B2B source SCU works as the B2B transfer master. The B2B target SCU is responsible for the phase measurement at the target ring. The source and target trigger SCUs are used to produce kicker trigger signals [19]. The calculation of the start of the synchronization window and the distribution of

it in the format of the timing message to the WR network is one of the tasks of the multi-purpose B2B source SCU. The timing message will be received by SCUs of the beam instrumentation and the corresponding devices will be activated by the timing message at the start time point of the synchronization window. In addition, the message will also be received by the trigger SCUs, indicating the synchronization window. Within the window, the first bucket indication signal will be selected plus a fixed delay to produce the trigger signals.

#### D. Basic Procedure

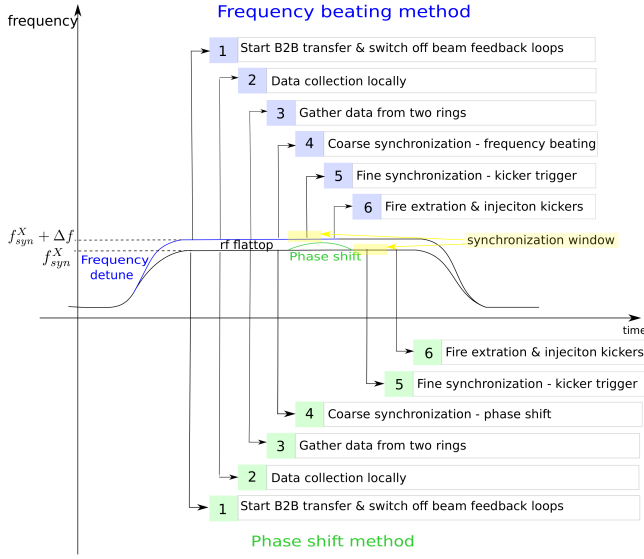


FIG. 9. Procedure of the B2B transfer within one acceleration cycle.

As illustrated here the procedure with the frequency beating method (blue, top) and that with the phase shift method (green, bottom).

Fig. 9 illustrates the basic procedure of the B2B transfer with the two different synchronization methods. The yellow region shows the synchronization window. The B2B transfer process basically needs to follow the six steps in Fig. 9 [19].

#### IV. BEAM DYNAMICS ANALYSIS OF TWO SYNCHRONIZATION METHODS

The FAIR B2B transfer system focuses first of all on the transfer from SIS18 to SIS100, so the beam dynamics of SIS18 beams are analyzed. Because the most stringent requirement are from the lightest and heaviest ion species, the beam dynamics of the  $H^+$  and  $U^{28+}$  beams are taken into consideration.

For the rf frequency modulation of the phase shift method ( $\Delta B/B = 0$ ), the dispersion function is reflected

in the relative momentum shift. The maximum tolerable relative momentum shift is decided by the semi-aperture  $a_H$  required for the beam, the lattice parameters (the envelope of the horizontal betatron oscillation  $\beta_H$  and the dispersion function  $D$ ) and the vertical beam emittance  $\varepsilon_H$  [20].

$$a_H(s) = \sqrt{\beta_H(s)\varepsilon_H} + |D(s) \cdot \frac{\Delta p}{p}| \quad (23)$$

By coincidence the maximum tolerable relative momentum of the  $H^+$  beam and that of the  $U^{28+}$  beam of the SIS18 are same,  $\Delta p/p_{max} = \pm 0.008$ .

For the frequency detuning of the frequency beating method ( $\Delta p/p = 0$ ), the dispersion function is reflected in the relative bending magnetic field shift.

$$a_H(s) = \sqrt{\beta_H(s)\varepsilon_H} + |D(s) \cdot \frac{\Delta B}{B}| \quad (24)$$

The maximum tolerable relative bending magnetic field shift of the  $H^+$  beam and that of the  $U^{28+}$  beam of the SIS18 are minus of their maximum tolerant relative momentum shift, namely  $\Delta B/B_{max} = -\Delta p/p_{max} = \pm 0.008$ . The constraint on the displacement of the orbit length  $\Delta L/L_{max}$  is obtained by

$$\frac{\Delta L}{L} = \begin{cases} \alpha_p \cdot \frac{\Delta p}{p} & \text{Phase shift method} \\ -\alpha_p \cdot \frac{\Delta B}{B} & \text{Frequency beating method} \end{cases} \quad (25)$$

$\alpha_p$  equals to 0.01 for the SIS18  $H^+$  beam and 0.03 for the SIS18  $U^{28+}$  beam [21].

The reasonable bucket size of a running bucket is larger than 80% of the size of a stationary bucket, namely the bucket area factor  $\alpha_b(\phi_s) \geq 80\%$ . Due to the constraint of the bucket size, the synchronous phase must stay within the range between  $-6.4^\circ$  and  $+6.4^\circ$  according to eq. 17.

The acceptable range of the parameters accompanying with the rf frequency modulation of the phase shift method for the SIS18  $H^+$  and  $U^{28+}$  beams are summarized in Tab. I and that accompanying with the frequency detuning of the frequency beating method are summarized in Tab. II. For detailed parameters of the SIS18 beams, please see Appendix B 1.

TABLE I. Acceptable range of the parameters accompanying with the rf frequency modulation of the phase shift method for the SIS18  $H^+$  and  $U^{28+}$  beams

$\Delta p/p_{max}$	$\Delta L/L_{max}$	$\alpha_b(\phi_s)_{min}$	$\phi_{s,max}$
$\pm 0.008$	$H^+ \pm 0.80 \cdot 10^{-4}$ $U^{28+} \pm 2.40 \cdot 10^{-4}$	80%	$\pm 6.4^\circ$

TABLE II. Acceptable range of the parameters accompanying with the frequency detune of the frequency beating method for the SIS18  $H^+$  and  $U^{28+}$  beams

$\Delta B/B_{max}$	$\Delta L/L_{max}$	$\alpha_b(\phi_s)_{min}$	$\phi_{s,max}$
$\pm 0.008$	$H^+ \pm 0.80 \cdot 10^{-4}$ $U^{28+} \pm 2.40 \cdot 10^{-4}$	80%	$\pm 6.4^\circ$

### A. Beam Dynamics of Phase Shift Method

In order to guarantee a bucket area factor larger than 80% and an adiabaticity smaller than  $10^{-4}$ , for the SIS18 200 MeV/u  $U^{28+}$  beam,  $|\Delta f_{rf}|$  must be smaller than 8.137 kHz and  $|\frac{d\Delta f_{rf}}{dt}|$  must be continuous and smaller than 95 Hz/ms and  $|\frac{d^2\Delta f_{rf}}{dt^2}|$  must be smaller than 70 Hz/ms<sup>2</sup> according to eq. 15, 16 and 18. Complied with the above mentioned criteria, the following three examples of rf frequency modulation profiles with a certain duration  $T$  are analyzed first of all for the SIS18  $U^{28+}$  beam. All three cases give the same phase shift of  $\pi$ . The phase shift is assumed to be achieved within 7 ms, namely  $T = 7$  ms.

Case (1) is a sinusoidal modulation.

$$\Delta f_1(t) = \frac{1}{2T} [1 - \cos(\frac{2\pi}{T}(t - t_0))] \quad (t_0 + 0, t_0 + T) \quad (26)$$

Case (2) is a parabolic modulation, which consists of three parabolas and two lines between every two parabolas.

$$\Delta f_2(t) = \begin{cases} \frac{9}{T^3}(t - t_0)^2 & (t_0 + 0, t_0 + \frac{T}{6}] \\ \frac{1}{4T} + \frac{3}{T^2}(t - t_0 - \frac{T}{6}) & (t_0 + \frac{T}{6}, t_0 + \frac{2T}{6}] \\ \frac{1}{T} - \frac{9}{T^3}(t - t_0 - \frac{T}{2})^2 & (t_0 + \frac{2T}{6}, t_0 + \frac{4T}{6}] \\ \frac{3}{4T} - \frac{3}{T^2}(t - t_0 - \frac{4T}{6}) & (t_0 + \frac{4T}{6}, t_0 + \frac{5T}{6}] \\ \frac{9}{T^3}(t - t_0 - T)^2 & (t_0 + \frac{5T}{6}, t_0 + T] \end{cases} \quad (27)$$

Case (3) is also a parabolic modulation, consisting of three parabolas.

$$\Delta f_3(t) = \begin{cases} \frac{8}{T^3}(t - t_0)^2 & (t_0 + 0, t_0 + \frac{T}{4}] \\ \frac{1}{T} - \frac{8}{T^3}[(t - t_0) - \frac{T}{2}]^2 & (t_0 + \frac{T}{4}, t_0 + \frac{3T}{4}] \\ \frac{8}{T^3}[T - (t - t_0)]^2 & (t_0 + \frac{3T}{4}, t_0 + T] \end{cases} \quad (28)$$

Fig. 10 shows three rf frequency modulation profiles and their 1<sup>st</sup> and 2<sup>nd</sup> time derivatives by Matlab. The corresponding beam dynamics parameters are illustrated in Fig. 11 and summarized in Tab. III.

According to the results, all three modulation profiles meet the requirements in Tab. I and keep the beam stable. However, compared with the parabolic modulation, the sinusoidal modulation has the smaller adiabaticity.

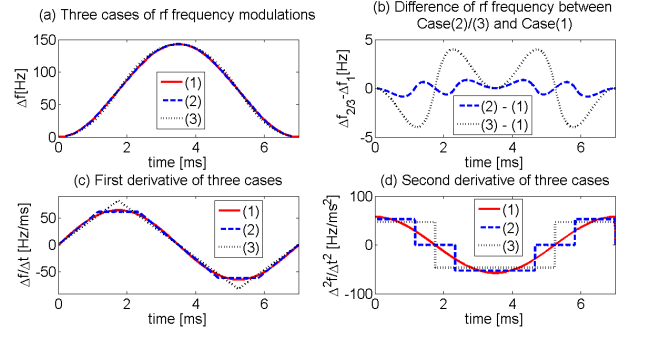


FIG. 10. Three rf frequency modulation cases. (a) three rf frequency modulation cases (b) difference between case (2)/(3) and case (1) (c) the 1<sup>st</sup> time derivative of three cases (d) the 2<sup>nd</sup> time derivative of three cases

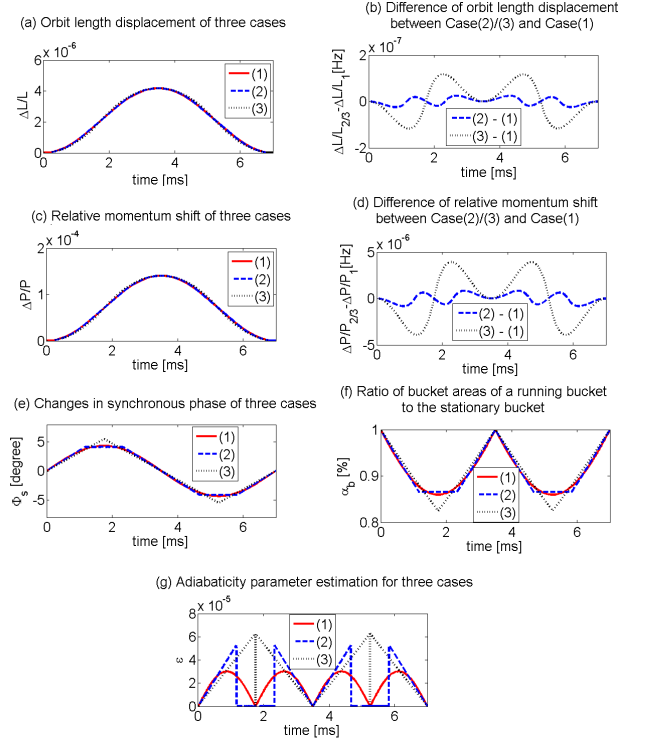


FIG. 11. Beam dynamics parameters of three cases. (a) orbit length displacement (b) difference of orbit length displacement between case (2)/(3) and case (1) (c) relative momentum shift (d) difference of relative momentum shift between case (2)/(3) and case (1) (e) changes in synchronous phase (f) ratio of bucket areas of a running bucket to the stationary bucket (g) adiabaticity

Hence, the sinusoidal modulation is preferable for the phase shift method. The sinusoidal rf frequency modulation for the SIS18 200 MeV/u  $U^{28+}$  needs 7 ms for the phase shift of  $\pi$ .

For SIS18, the chromaticities  $Q_x^i$  and  $Q_y^i$  for the  $U^{28+}$  operation are  $-6.5$  and  $-4.1$ . Using the chromaticity and the maximum momentum shift (see. Tab. III), the chromatic tune shifts  $\Delta Q_x$  and  $\Delta Q_y$  during rf modulations



TABLE III. Corresponding beam dynamics parameters of three cases

	Case (1)	Case (2)	Case (3)
Maximum orbit length displacement	$4.18 \cdot 10^{-6}$	$4.18 \cdot 10^{-6}$	$4.18 \cdot 10^{-6}$
Maximum relative momentum shift	$1.40 \cdot 10^{-4}$	$1.40 \cdot 10^{-4}$	$1.40 \cdot 10^{-4}$
Synchronous phase	$< \pm 6.4^\circ$	$< \pm 6.4^\circ$	$< \pm 6.4^\circ$
Minimum bucket area factor	86.0%	86.5%	82.5%
Maximum adiabaticity	$3.0 \cdot 10^{-5}$	$5.90 \cdot 10^{-5}$	$6.30 \cdot 10^{-5}$

for three cases are calculated as

$$\Delta Q_x = Q'_x \frac{\Delta p}{p} = -6.5 \cdot 1.40 \cdot 10^{-4} = -9.10 \cdot 10^{-4} \quad (29)$$

$$\Delta Q_y = Q'_y \frac{\Delta p}{p} = -4.1 \cdot 1.40 \cdot 10^{-4} = -5.74 \cdot 10^{-4} \quad (30)$$

The chromatic tune shifts for three cases are negligible.

For the SIS18 4 GeV/u  $H^+$  beam,  $|\Delta f_{rf}|$  must be smaller than 283 Hz and  $|\frac{d\Delta f_{rf}}{dt}|$  must be continuous and smaller than 1.9 Hz/ms and  $|\frac{d^2\Delta f_{rf}}{dt^2}|$  must be smaller than 0.2 Hz/ms<sup>2</sup> according to eq. 15, 16 and 18. With regard to these criteria, the sinusoidal modulation with  $T = 50$  ms is used for the phase shift of  $\pi$ . The corresponding beam dynamics parameters are in Tab. IV.

TABLE IV. Parameters accompanying with a 50 ms sinusoidal modulation for the SIS18  $H^+$  beam

Maximum orbit length displacement	Maximum Relative momentum shift	Synchronous phase	Minimum bucket area factor	Maximum adiabaticity
$5.70 \cdot 10^{-6}$	$5.70 \cdot 10^{-4}$	$< \pm 4.2^\circ$	86%	$0.80 \cdot 10^{-4}$

For the frequency modulation of the SIS18  $H^+$  beam, a longer period sinusoidal modulation (e.g. 50 ms) must be used for the beam performance consideration. For the SIS18  $H^+$  beam, the chromaticity  $Q'_x$  and  $Q'_y$  of  $H^+$  is  $-7.5$  and  $-4.4$ . Using the chromaticity and the maximum momentum shift (see. Tab. IV), the maximum chromatic tune shift  $\Delta Q_x$  and  $\Delta Q_y$  for the 50 ms sinusoidal modulation are calculated as

$$\Delta Q_x = Q'_x \frac{\Delta p}{p} = -7.5 \cdot 5.7 \cdot 10^{-4} = -4.28 \cdot 10^{-3} \quad (31)$$

$$\Delta Q_y = Q'_y \frac{\Delta p}{p} = -4.4 \cdot 5.7 \cdot 10^{-4} = -2.51 \cdot 10^{-3} \quad (32)$$

For the SIS18 4 GeV/u  $H^+$  beam, the chromatic tune shifts for the 50 ms sinusoidal modulation are negligible.

The investigation of the phase shift performance based on the experiments carried out in the Proton Synchrotron (PS) at CERN is presented in the article [22].

## B. Beam Dynamics of Frequency Beating Method

The frequency detuning has no influence on the chromaticity tune shift, because the momentum of the synchronous particle is not affected by the frequency detuning in order to guarantee the match of the extraction and injection energy.

For the frequency beating method, the rf frequency detuning is done at the end of the SIS18 rf acceleration ramp. The SIS18  $U^{28+}$  and  $H^+$  acceptable displacement of the orbit length is  $\pm 2.4 \cdot 10^{-4}$  and  $\pm 0.80 \cdot 10^{-4}$ , see Tab. II. Hence, the tolerable rf frequency change for 200 MeV/u  $U^{28+}$  and 4 GeV/u  $H^+$  is calculated as

$$\frac{\Delta f_{rf}}{f_{rf}} = -\frac{\Delta L}{L} = \begin{cases} \mp 2.4 \cdot 10^{-4} & U^{28+} \\ \mp 0.80 \cdot 10^{-4} & H^+ \end{cases} \quad (33)$$

where the maximum rf frequency detuning approximates to 377 Hz and 109 Hz for the 200 MeV/u  $U^{28+}$  and 4 GeV/u  $H^+$  beams.

## V. TIMING CONSTRAINTS

The FAIR B2B transfer system has strict timing constraints. Because beam feedback loops (e.g. the beam phase control loop, the bunch-by-bunch longitudinal feedback loop [4]) must be switched-off before the B2B transfer, which modify the rf system according to the actual beam, the beam may be stable only for a short period of time. For most FAIR use cases, the upper bound time of the B2B transfer process is 10 ms.

The complete phase measurement needs approximately 500  $\mu$ s. The longer time is used for the phase measurement, the more precise the measurement result will be [23]. The upper bound B2B related message transfer latency on the WR network is defined as 500  $\mu$ s. So the transfer latency of the phase measurement from the B2B target SCU to the B2B source SCU is 500  $\mu$ s in the worst case. The B2B source SCU needs about 100  $\mu$ s for the data calculation, message creation and sending. The timing message containing the start of the synchronization window needs a 500  $\mu$ s transfer latency on the network to the DM and another 500  $\mu$ s further to SCUs responsible for beam instrumentation devices. Bunches must be transferred after beam instrumentation devices are activated. Hence, the start of the synchronization window must be  $2 \cdot 500 \mu\text{s} + 100 \mu\text{s} + 2 \cdot 500 \mu\text{s} = 2.1$  ms later than the start of the B2B transfer process.

In the following part, the WR network is characterized for the B2B transfer to meet the 500  $\mu$ s timing constraint and the running time of the B2B related firmware running on the soft CPU, Latticemico32, of the SCU is checked for the timing constraints of 100  $\mu$ s.

#### A. Characterization of the WR Network for the B2B Transfer

In order to meet the timing constraint of the B2B transfer, the data transfer on the WR network has an upper bound transfer latency of 500  $\mu$ s, 400  $\mu$ s of which can be used for the network transfer. Hence, the maximum number of WR switch layers between the B2B related SCUs must be defined. Meanwhile, more switches require more optical fiber connections. The optical fiber connections cause the bit error of the frame. These frames will be discarded by switches. Therefore, the maximum number of WR switch layers is constrained not only by the transfer latency, but also by the tolerable lost frames. The lost frame caused by bit errors is measured by the frame error rate (FER), which is defined as the ratio between the number of lost frames caused by bit errors and the number of sent frames. The FER is calculated as [24]

$$FER = n \cdot 10^{-12} \cdot 880 \quad (34)$$

where  $n$  is the number of WR switches used to establish the communication and the optical fiber's bit error rate [25] specified by the manufactures is  $10^{-12}$  [26] and 880 is the length of a timing message in the unit of bit [27].

For the B2B transfer, there are two types of messages. The 1<sup>st</sup> type message is used to exchange data between two rings, which is sent by one SCU and sent to all other B2B related SCUs, e.g. the message of the phase measurement. The bandwidth is 25 kbit/s. The 2<sup>nd</sup> type message is used to transfer data to the DM, which is sent by one SCU and sent only to the DM, e.g. the message of the start of the synchronization window. The bandwidth is 5 kbit/s [19]. Both the two types have the same format as the timing message with the length of 110 bytes. The tolerable FER is defined as one lost frame during a certain duration and calculated as

$$tolerable\_FER = \frac{1}{bandwidth \cdot duration} \cdot 880 \quad (35)$$

The requirements for these two type messages are listed here.

In the test, the Xena's Layer 2-3 test platform was used to characterize the properties of the WR network for the B2B transfer. The Xena's Layer 2-3 test platform was used to configure and generate Ethernet traffic at the data link layer and network layer and then to analyze how WR network in response. Fig. 12 shows an overview of the Xena's Layer 2-3 test platform for the WR network. The test platform used the 4U XenaBay chassis which

TABLE V. Requirements for the two B2B types messages

	Maximum latency	Tolerable FER	Remark
1 <sup>st</sup> type	400 $\mu$ s	$6.70 \cdot 10^{-9}$	One lost frame every two months
2 <sup>nd</sup> type	400 $\mu$ s	$1.34 \cdot 10^{-9}$	

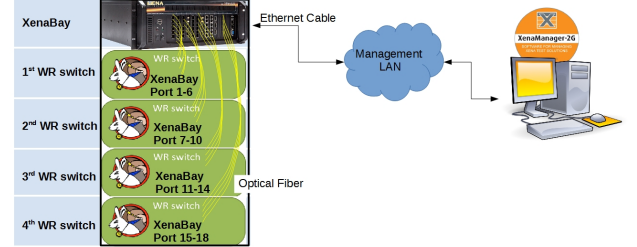


FIG. 12. An overview of the Xena's Layer 2-3 test platform for the WR network.

was equipped with an extensive range of copper and optical Gigabit Ethernet test modules. In the test, the test modules used 18 AXGE-1254 transceivers, 1.25 Gbps single fiber bidirectional small form-factor pluggable (SFP), to connect to ports of four WR switches via a G.652.B type single mode fibers. The chassis and test modules were controlled via Xena Manager-2G, a free Windows GUI client, which can be used to manage test equipment and execute test remotely. The test is used to identify the tolerable number of WR switch layers for the B2B transfer.

According to the importance of the network traffic, the prioritization of WR network traffic is implemented based on the virtual LAN (VLAN) technology. Control messages must be delivered deterministically and with very low loss, which schedules the real-time acceleration cycle. Hence, they are assigned to a VLAN with the highest priority, as well as the 2<sup>nd</sup> type B2B message. Besides, messages used for the B2B related data exchange are assigned to a specific B2B VLAN with the secondary priority in order to reduce the network traffic. In addition, management messages are assigned to another VLAN with the lowest priority [28]. For more details of the traffic produced by XenaBay ports, please see Appendix A.

The 1<sup>st</sup> type B2B messages are produced by one XenaBay's port and transferred via all four WR switches. After each switch, messages are received by another XenaBay's port. The transfer latency of the message via different number of switch layers is measured. Tab. VI shows the 45 days test result [28].

The 2<sup>nd</sup> type B2B messages are produced by one XenaBay's port and transferred via all four WR switches to another XenaBay's port. The transfer latency of the message via four switch layers, 23  $\mu$ s, is measured in the 45 days test [28].

TABLE VI. Maximum frame transfer latency of the 1<sup>st</sup> type B2B messages

Number of switch layers	one	two	three	four
Maximum transfer latency	28 $\mu$ s	34 $\mu$ s	37 $\mu$ s	41 $\mu$ s

Based on the transfer latency requirement, the tolerable number of switch layers for the 1<sup>st</sup> and 2<sup>nd</sup> type B2B messages are calculated as

$$\frac{400 \mu\text{s}}{28 \mu\text{s}} > 13 \quad (36)$$

$$\frac{400 \mu\text{s}}{23 \mu\text{s}} \cdot 4 > 67 \quad (37)$$

According to the tolerable FER requirement, the maximum number of switch layers for the two types are calculated by eq. 34.

$$n_{1st} = \frac{FER}{880 \cdot 10^{-12}} = \frac{6.70 \cdot 10^{-9}}{880 \cdot 10^{-12}} \approx 8 \quad (38)$$

$$n_{2nd} = \frac{FER}{880 \cdot 10^{-12}} = \frac{1.34 \cdot 10^{-9}}{880 \cdot 10^{-12}} \approx 38 \quad (39)$$

The tolerable FER requires less number of WR switch layers compared with the result from the transfer latency requirement. Hence, the maximum number of switch layers for the two type messages are 8 and 38, when one lost B2B related frame is tolerable every two months.

### B. Firmware Running on LM32

The test setup was used to check whether the B2B firmware running on the LM32 of the SCUs meets the time constraints of the B2B transfer system.

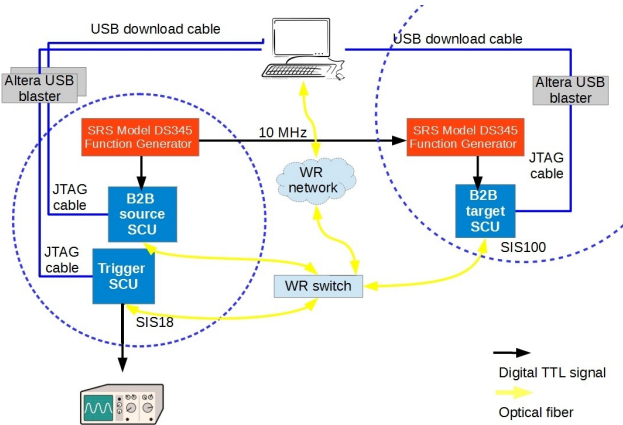


FIG. 13. Schematic of the test setup.

Fig. 13 shows the schematic of the test setup. In this test setup, two SRS MODEL DS345 Synthesized Function Generators (short: DS345) were used to simulate the rf systems of the SIS18 and SIS100. The two DS345s needed to be synchronized to a common reference clock. For simplicity, the DS345 of the SIS100 used a 10 MHz clock from the DS345 of the SIS18 as an external reference clock. The B2B source SCU, the B2B target SCU and the Trigger SCU were connected to a WR switch via single mode fibers, which connected to the WR network. A personal computer (PC) was connected to the WR network, which was a Linux PC installed with the FEC tools, the Altera's Quartus II software and the pack-ETH software. The SCUs were connected to the PC via the Altera USB-Blaster Joint Test Action Group (JTAG) programmer. The PC was used to simulate the DM to produce the B2B start timing message by the packETH software. Besides, the PC monitored the status of the firmware in all SCUs and measured the running time of the firmware by the SignalTap II Logic Analyzer feature within the Quartus II software. Two DS345s outputted signals to an oscilloscope, together with an output signal from the trigger SCU. Fig. 14 shows the front view of the test setup.

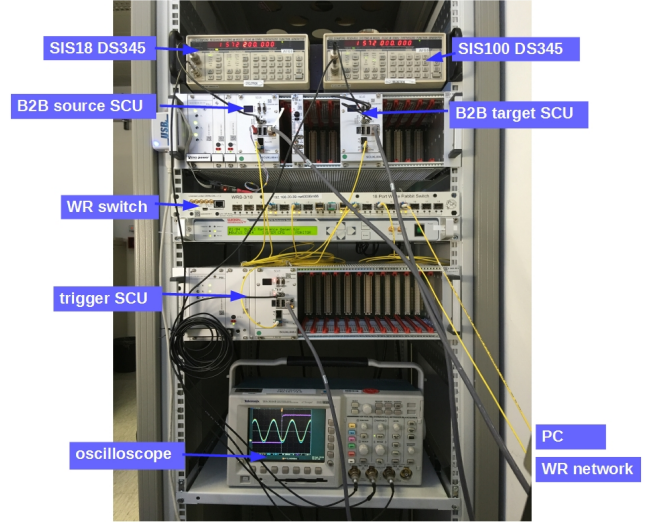


FIG. 14. Front view of the test setup.

From the functional perspective, the B2B source and target SCUs measured the phase of the signals from two DS345, after they received the B2B start timing message from the PC. Then the measured phase value of the target ring was transferred from the B2B target SCU to the B2B source SCU. After receiving the message containing the measured phase value, the B2B source SCU calculated the start of the synchronization window and then distributed the start of the synchronization window to the trigger SCU via the WR network. When the trigger SCU received the message containing the start of the synchronization window, it produced a TTL signal output to the oscilloscope, indicating the phase alignment of

the two signals from the DS345s. During the process, the running time of some tasks of the firmware was measured by the SignalTap II Logic Analyzer, see Tab. VII.

TABLE VII. Task running time of the firmware on LM32 of the B2B source SCU

Task	Average running time	Worst-case running time
Timing message detection	336 ns	336 ns
Timing message reading	2.7 $\mu$ s	2.7 $\mu$ s
Calculation the synchronization window	12.6 $\mu$ s	12.8 $\mu$ s
Timing message sending	3.2 $\mu$ s	3.2 $\mu$ s

According to the measured task running time results, the total time consumption on the source SCU is shorter than 20  $\mu$ s, 20% of 100  $\mu$ s. Hence, the B2B firmware running on LM32 meets the timing constraints of the B2B transfer.

## VI. APPLICATION

For the FAIR B2B transfer system, both the phase shift and frequency beating methods are applicable. However, many FAIR accelerator pairs can only use the frequency beating method because of the non-integer ratio of the circumference between two rings. Besides, FAIR has many use cases of the B2B transfer that the extraction and injection beam have different energy because of targets installed between two rings. In this case, the beam revolution frequency ratio between the small and large accelerators is used to calculate the synchronization frequencies instead of the circumference ratio between the large and small accelerators. Therefore, the FAIR B2B transfer system with the frequency beating method is applied for all FAIR use cases, see Tab. VIII.

Tab. VIII shows that for most primary beam transfers of FAIR use cases, the B2B transfer with the B2B injection center mismatch less than  $\pm 1^\circ$  can be achieved, because the circumference ratio between two rings is an integer or close to an integer. For the B2B transfer between two rings with a far away circumference ratio, the B2B injection center mismatch is  $\pm 1.2^\circ$ , which is just beyond the specification and still acceptable. However, the system is also required for the FAIR use cases that secondary beams are generated by the pbar target, the FRS or the Super-FRS with an arbitrary energy ratio between the primary and secondary beams. For the rare isotope beam (RIB) transfer from the SIS100 to the CR via the Super-FRS with the 1.5 GeV/u primary beam energy and the 740 MeV/u secondary beam energy, the B2B injection center mismatch is only  $\pm 2.1^\circ$  by coincidence. For the antiproton B2B transfer from the SIS100 to the CR via the pbar target and the RIB transfer from the

SIS18 to the ESR via the FRS, the B2B injection center mismatch is as large as  $\pm 41.5^\circ$ , which is far beyond the upper bound injection center mismatch. For detailed parameters of the FAIR B2B transfer use cases, please see Appendix. B

Fig. 15 shows the positive B2B injection center mismatch of the RIB B2B transfer from the SIS100 to the CR via the Super-FRS with the different primary and secondary beam energies. The negative mismatch is just the additive inverse of the positive mismatch. Fig. 16 shows the positive mismatch of the proton B2B transfer from the SIS100 to the CR via the pbar target and Fig. 17 shows the positive mismatch of the beam transfer from the SIS18 to the ESR via the FRS.

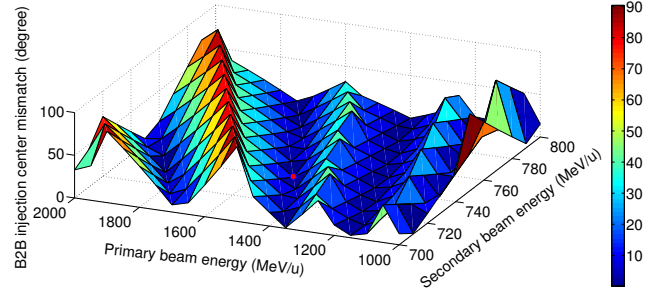


FIG. 15. Positive B2B injection center mismatch of the RIB B2B transfer from the SIS100 to the CR via the Super-FRS with the different primary and secondary beam energies.

*Red dot is the mismatch in the case of the 1.5 GeV/u primary beam energy and the 740 MeV/u secondary beam energy.*

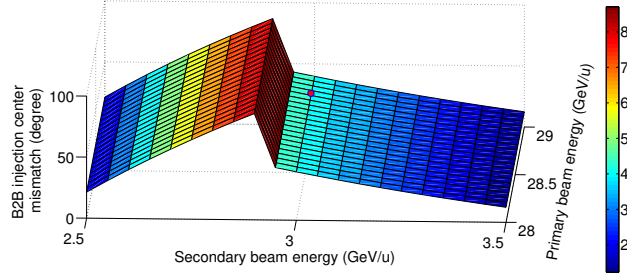


FIG. 16. Positive B2B injection center mismatch of the proton B2B transfer from the SIS100 to the CR via the pbar target with the different primary and secondary beam energies.

*Red dot is the mismatch in the case of the 28.8 GeV/u primary beam energy and the 3 GeV/u secondary beam energy.*

## VII. CONCLUSION

The concept of the FAIR B2B transfer system and its application for all FAIR use cases were presented, as well as the systematic investigation from the timing and the

TABLE VIII. Application of the FAIR B2B transfer system for FAIR accelerators with the frequency beating method

No.	FAIR use cases	$C^l/C^s$	$f_{rev}^s/f_{rev}^l$	$f_{syn}^{src}$	$f_{syn}^{trg}$	$f_{bucket}$	B2B injection center mismatch	Remark
1	Four batches, each of two SIS18 $U^{28+}$ bunches (200 MeV/u) $\rightarrow$ eight out of ten SIS100 buckets	5 (200Hz detune for $f_{rf}^{SIS18}$ )		$2f_{rev}^{SIS18}$	$10f_{rev}^{SIS100}$	$f_{rev}^{SIS100}$	$\pm 0.4^\circ$	The FAIR use cases 1-5 have the B2B injection center mismatch smaller than the upper bound $\pm 1^\circ$ , because the circumference ratio between two rings is an integer or close to an integer.
2	Four batches, each of one SIS18 $H^+$ bunch (4 GeV/u) $\rightarrow$ four out of ten SIS100 buckets	5 (200Hz detune for $f_{rf}^{SIS18}$ )		$f_{rev}^{SIS18}$	$5f_{rev}^{SIS100}$	$f_{rev}^{SIS100}$	$\pm 0.4^\circ$	
3	Two of four SIS18 bunches (30 MeV/u) $\rightarrow$ two ESR buckets	2-0.003		$4f_{rev}^{SIS18}$	$2f_{rev}^{ESR}$	$f_{rev}^{ESR}$	$\pm 0.5^\circ$	
4	One SIS18 $H^+$ bunch (400 MeV/u) $\rightarrow$ one ESR bucket	2-0.003		$f_{rev}^{SIS18}$	$f_{rev}^{ESR}/2$	$f_{syn}^{ESR}$	$\pm 0.5^\circ$	
5	One ESR bunch (30 MeV/u) $\rightarrow$ one CRYRING bucket	2-0.003		$f_{rev}^{ESR}$	$f_{rev}^{CRYRING}/2$	$f_{syn}^{CRYRING}$	$\pm 0.5^\circ$	
6	One CR antiproton bunch (3 GeV/u) $\rightarrow$ one HESR bucket	2.6-0.003		$f_{rev}^{CR}/13$	$f_{rev}^{HESR}/5$	$f_{syn}^{HESR}$	$\pm 1.2^\circ$	The B2B injection center mismatch is just beyond the specification, but it is still acceptable. Although the circumference ratio between two rings is far away from an integer.
7	One CR RIB bunch (740 MeV/u) $\rightarrow$ one HESR bucket	2.6-0.003		$f_{rev}^{CR}/13$	$f_{rev}^{HESR}/5$	$f_{syn}^{HESR}$	$\pm 1.2^\circ$	
8	One SIS100 $H^+$ bunch (28.8 GeV/u) $\xrightarrow{\text{pbar target}}$ $H^-$ (3 GeV/u) one CR bucket	not applicable	$4.8 - 0.041$	$f_{rev}^{SIS100}/5$	$f_{rev}^{CR}/24$	$f_{syn}^{CR}$	$\pm 41.5^\circ$	The B2B injection center mismatch is far beyond the specification, because the energy ratio before and after targets is arbitrary. (The FAIR use case No. 9 is close to the specification and still acceptable by coincidence.)
9	One SIS100 heavy ion bunch (1.5 GeV/u) $\xrightarrow{\text{Super-FRS}}$ RIB (740 MeV/u) one CR bucket	not applicable	$4.4 - 0.0046$	$f_{rev}^{SIS100}/5$	$f_{rev}^{CR}/11$	$f_{syn}^{CR}$	$\pm 2.1^\circ$	
10	One SIS18 heavy ion bunch (550 MeV/u) $\xrightarrow{\text{FRS}}$ RIB (400 MeV/u) one ESR bucket	not applicable	$1.8 + 0.036$	$f_{rev}^{SIS18}/5$	$f_{rev}^{ESR}/9$	$f_{syn}^{ESR}$	$\pm 31.2^\circ$	

beam dynamics perspectives. The new FAIR B2B transfer system fulfills the requirements for FAIR.

For the B2B transfer from the SIS18 to the SIS100 with the phase shift method, the sinusoidal rf frequency modulation is a better choice compared with the same periodical parabolic modulation. It needs 7 ms for the SIS18 200 MeV/u  $U^{28+}$  and 50 ms for the SIS18 4 GeV/u  $H^+$  to achieve the phase shift of  $\pi$  in order to guarantee

a bucket area factor larger than 80% and an adiabaticity smaller than  $10^{-4}$ .

Two test setups were built to verify the timing constraints. The first test setup was used to characterize the WR network for the B2B transfer. If for instance one lost frame is tolerable every two month, the maximum 38 WR switch layers can be used between the B2B related SCUs and the DM and the maximum 8 WR switch layers



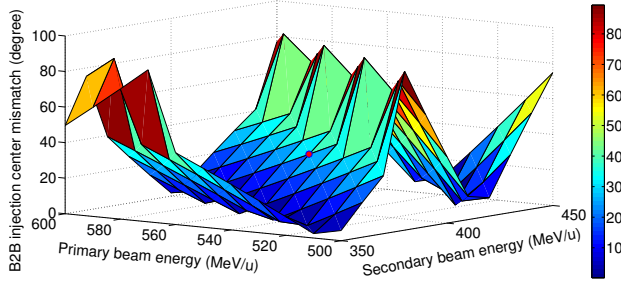


FIG. 17. Positive B2B injection center mismatch of the beam transfer from the SIS18 to the ESR via the FRS with the different primary and secondary beam energies.

Red dot is the mismatch in the case of an operation mode with the 550 MeV/u primary beam energy and the 400 MeV/u secondary beam energy.

can be used between the B2B related SCUs. In the second test setup, the firmware of the FAIR B2B transfer system was evaluated, running on the soft CPU, LatticeMico32, of the SCUs. The measurement results show that the firmware running on the LatticeMico32 of the SCUs meets the requirement of the timing constraints.

For all primary beam transfers of FAIR use cases, the B2B injection center mismatch within  $\pm 1.2^\circ$  is accept-

able. However, for the FAIR use cases of the secondary beams, the mismatch is as large as  $\pm 41.5^\circ$ .

The most important investigations for the FAIR B2B transfer system were discussed in this manuscript. However, there are still some investigations which are required for the final system operation. The magnetic horn after the pbar target has to be synchronized with the antiproton beam to the “us” order of magnitude. The bunch compressor of the SIS100 has to be synchronized the beam extraction. Finally, for the FAIR use cases of the secondary beam with the B2B injection center mismatch larger than  $\pm 41.5^\circ$ , the FAIR B2B transfer system with specific beam accumulation methods (e.g. the barrier bucket or the unstable fixed point accumulation) has to be checked.

The realistic test of the system on FAIR accelerators will be done at the end of 2018, because many FAIR technical basis and rings are still under construction.

## VIII. ACKNOWLEDGMENTS

The author would like to express the sincere gratitude to colleagues from the CSCO and PBRF departments, GSI, for their technical support. The gratitude also extends to colleagues from the SBES, PBHV, SHE-P departments, GSI.

- 
- [1] J. Eschke. International Facility for Antiproton and Ion Research (FAIR) at GSI, Darmstadt. *Journal of Physics G: Nuclear and Particle Physics*, 31(6):S967, 2005. URL <http://iopscience.iop.org/article/10.1088/0954-3899/31/6/041/meta>.
  - [2] FAIR - Facility for Antiproton and Ion Research, 2011. URL <https://www.gsi.de/forschungbeschleuniger/fair.htm>.
  - [3] P. Moritz. BuTiSDevelopment of a Bunchphase Timing System. *GSI Scientific Report*, 2006. URL <http://citeseerx.ist.psu.edu/viewdoc/download?doi=10.1.1.162.1765&rep=rep1&type=pdf>.
  - [4] H. Klingbeil and et al. New Digital Low-Level RF System for heavy-ion Synchrotrons. *Physical Review Special Topics - Accelerators and Beams*, 14(10), 2011. ISSN 1098-4402. doi:10.1103/PhysRevSTAB.14.102802. URL <http://link.aps.org/doi/10.1103/PhysRevSTAB.14.102802>.
  - [5] P. Moritz. F-CS-RF-14e BuTiS, Common Specification on the Bunch Phase Timing System (BuTiS). *FAIR Common Specification*, 2012.
  - [6] D. Beck and et al. The General Machine Timing System for FAIR and GSI. *GSI Internal Document*, 2013. URL [https://www-acc.gsi.de/wiki/pub/Timing/TimingSystemDocuments/GMT\\_Description\\_v3-1.pdf](https://www-acc.gsi.de/wiki/pub/Timing/TimingSystemDocuments/GMT_Description_v3-1.pdf).
  - [7] D. Beck and et al. White Rabbit Technology as Basis for the FAIR Timing System. *GSI Scientific Report*, 2011. URL <https://www-acc.gsi.de/wiki/pub/Timing/TimingSystemDocuments/PHN-ACC-RD-45.pdf>.
  - [8] R. Garoby. CERN-PS-RF-NOTE-84-6, Timing Aspect of Bunch Transfer between Circular Machines: State of the Art in the PS Complex. *CERN Internal Publication*, 1984.
  - [9] CERN accelerator complex, . URL <https://home.cern/about/accelerators>.
  - [10] H. Damerau. Lecture Note: Timing, Synchronization & Longitudinal Aspects. *CERN Accelerator School*, 2017. URL <https://cas.web.cern.ch/cas/IET2017/Lectures/DamerauI.pdf>.
  - [11] T. Ferrand, H. Klingbeil, and H. Damerau. CERN-ACC-NOTE-2015-0025, Synchronization of Synchrotrons for Bunch-to-Bucket Transfers. *CERN Internal Publication*, 2015. URL <http://cds.cern.ch/record/2053285>.
  - [12] P. Baudrenghien, T. Linnecar, D. Stellfeld, and U. Wehrle. SPS Beams for LHC: RF Beam Control To Minimize Rephasing In The SPS. In *Proc. of EPAC*, pages 22–26, 1998. URL <http://www.cern.ch/accelconf/e98/PAPERS/WEPO2H.PDF>.
  - [13] D. Beck and et al. The new White Rabbit based Timing System for the FAIR Facility. In *Proc. of PCaPAC*, Kolkata, India, 2012. URL <http://accelconf.web.cern.ch/Accelconf/pcapac2012/papers/fria01.pdf>.
  - [14] K. Kaiser. F-TN-C-008e, Detailed Documentation of the Scalable Control Unit SCU3 FG 900.112. *FAIR Technical Note*, 2014.
  - [15] H. Klingbeil. Detailed Specification on the LLRF DSP System for FAIR Ring RF Systems. *GSI Internal Document*, 2013.

- [16] C. Bovet, R. Gouiran, K.H. Reich, and I. Gumowski. A Selection Of Formula And Data Useful For The Design Of AG Synchrotrons. Technical report, CERN, 1970. URL <http://cds.cern.ch/record/280305/files/cm-p00041563.pdf>.
- [17] S. Y. Lee. *Accelerator Physics*. WORLD SCIENTIFIC, Singapore, 3 edition, 2011. ISBN 978-981-4374-94-1 978-981-4374-95-8. URL <http://www.worldscientific.com/worldscibooks/10.1142/8335>.
- [18] E. Ezura, M. Yoshii, F. Tamura, and A. Schnase. Beam-Dynamics View of RF Phase Adjustment for Synchronizing J-PARC RCS with MR or MLF. *KEK Internal Document*, 2008.
- [19] J. Bai and T. Ferrand. F-TC-C-05, Concept of the FAIR Bunch To Bucket Transfer System. *FAIR Technical Concept*, 2016.
- [20] E. J. N. Wilson. Lecture Note: Transverse Motion. *CERN Accelerator School*, 2005. URL <http://cds.cern.ch/record/1058077/files/p17.pdf>.
- [21] H. Liebermann and D. Ondreka. FAIR and GSI Reference Cycles for SIS18. *GSI Internal Document*, 2013.
- [22] T. Ferrand and et al. RF Phase Shift Beam Synchronization for FAIR. *Manuscript submitted for publication*, 2018.
- [23] T. Ferrand. *Development of the LLRF System for a Deterministic Bunch-to-Bucket Transfer for FAIR*. (Unpublished doctoral thesis), Technical University Darmstadt, Germany.
- [24] C. Prados and M. Lipinski. White Rabbit and Robustness, 2011. URL <http://www.ohwr.org/documents/103>.
- [25] Note1. Bit error rate: the number of bit errors divided by the total number of transferred bits during a studied time interval.
- [26] Datasheet of Draka Optical fiber, . URL <http://www.drakauc.com/ucfibre-optical-patchcords/>.
- [27] D. Beck. Timing Messages of GMT System for FAIR, 2015. URL <https://www-acc.gsi.de/wiki/Timing/TimingSystemEvent>.
- [28] C. Prados and J. Bai. Testing the WR Network of the FAIR General Machine Timing System. *GSI Internal Document*, 2016.

## Appendix A: Traffic produced by the XenaBay ports of the test setup

TABLE IX. Traffic produced by the XenaBay ports of the test setup

Adapted from “Testing the WR Network of the FAIR General Machine Timing System” by C. Prados and J. Bai, 2016, GSI Internal Document.

Switch	XenaBay Port	Traffic	Ethernet frame size (bytes)	VLAN	Priority	Usage
WR switch 1	Port 1	100 Mbit/s	110	7	7	Control message Broadcast
	Port 2					
	Port 3	10 Mbit/s	110	7	7	Control message Unicast
	Port 4					
	Port 5					
	Port 6	1 Mbit/s	64 - 1518	5	5	Management Broadcast
WR switch 2	Port 7	2 Mbit/s	64 - 1518	5	5	Management Broadcast
	Port 8					
	Port 9					
	Port 10	1 Mbit/s	64 - 1518	5	5	Management Broadcast
WR switch 3	Port 11					
	Port 12					
	Port 13	2 Mbit/s	64 - 1518	5	5	Management Broadcast
	Port 14	1 Mbit/s	64 - 1518	5	5	Management Broadcast
WR switch 4	Port 15	1 Mbit/s	64 - 1518	5	5	Management Broadcast
	Port 16	25 kbit/s	110	6	6	B2B Broadcast
	Port 17	5 kbit/s	110	7	7	B2B Unicast
	Port 18	2 Mbit/s	64 - 1518	5	5	Management Broadcast
Broadcast: messages are sent by one port and sent to all other ports. Unicast: messages are sent by one port and sent to a specific port.						

## Appendix B: Parameters of FAIR B2B transfer use cases

### 1. Parameters of the B2B Transfer from SIS18 to SIS100

TABLE X: Parameters related to the B2B transfer from the SIS18 to the SIS100

	Unit	Proton		Heavy Ion $U^{28+}$	
		SIS18 Ext	SIS100 Inj	SIS18 Ext	SIS100 Inj
Design orbit	m	216.72	1083.6	216.72	1083.6
$C_{SIS18} : C_{SIS100}$		5		5	
Ext kinetic energy	MeV/u	4000		200	
Inj kinetic energy	MeV/u		4000		200
h		1	10(1×4)	2	10(2×4)
$f_{rf}$	MHz	1.359358	2.718715	1.572536	1.572536
$T_{rf}$	μs	0.736	0.368	0.636	0.636
$f_{rev}$	MHz	1.359358	0.271872	0.786268	0.157254
$T_{rev}$	μs	0.736	3.678	1.272	6.359
Max $\Delta p/p$		±0.008	±0.01	±0.008	±0.01
$\Delta R/R$		±0.8 × 10 <sup>-4</sup>		±2.4 × 10 <sup>-4</sup>	
$\eta = \frac{1}{\gamma^2} - \alpha_p$		0.026		0.647	
$\gamma_t$		10		5.8	
$\alpha_p$		0.010		0.030	
$\beta$		0.982	0.982	0.568	0.568
$\gamma$		5.294	5.294	1.215	1.215
$Q_x$		4.17		4.17	
$Q_y$		3.4		3.4	
$Q_x$		-7.5		-6.5	

$Q_y$		-4.4		-4.1	
		Injection four times		Injection four times	

## 2. Parameters of the B2B Transfer from SIS18 to ESR

TABLE XI: Parameters related to the B2B transfer from the SIS18 to the ESR

		Proton/Heavy Ion		Heavy Ion	
	Unit	SIS18 Ext	ESR Inj	SIS18 Ext	ESR Inj
Design orbit	m	216.72	108.36	216.72	108.36
Inj orbit	m		108.36+0.15		108.36+0.15
$C_{SIS18} : C_{ESR}$		1.997		1.997	
Ext kinetic energy	MeV/u	550		30	
Inj kinetic energy	MeV/u		400		30
h		1	1	4	2
$f_{rf}$	MHz	0.989756	1.976777	1.373201	1.371302
$T_{rf}$	$\mu$ s	1.010	0.506	0.728	0.879
$f_{rev}$	MHz	0.989756	1.976777	0.343300	0.685651
$T_{rev}$	$\mu$ s	1.010	0.506	2.913	1.458
$\Delta p/p$ compared with design orbit			1%		1%
$\Delta R/R$			0.138%		0.138%
$\eta = \frac{1}{\gamma^2} - \alpha_p$		0.480	0.310	0.909	0.759
$\gamma_t$		10	2.357	5.8	2.357
$\alpha_p$		0.010	0.18	0.030	0.18
$\beta$		0.715	0.715	0.248	0.248
$\gamma$		1.429	1.429	1.032	1.032
		Accumulation beam in injection orbit		Accumulation beam in injection orbit	

## 3. Parameters of the B2B Transfer from SIS18 to ESR via the FRS

TABLE XII: Parameters related to the B2B transfer from the SIS18 to the ESR via the FRS

		Heavy Ion Beam	Rare Isotope Beam
	Unit	SIS18 Ext	ESR Inj
Design orbit	m	216.72	108.36
Inj orbit	m		108.36+0.15
$C_{SIS18} : C_{ESR}$		1.997	
Ext kinetic energy	MeV/u	550	
Inj kinetic energy	MeV/u		400
h		1	1
$f_{rf}$	MHz	1.076965	1.976777
$T_{rf}$	$\mu$ s	0.929	0.506
$f_{rev}$	MHz	1.076965	1.976777
$T_{rev}$	$\mu$ s	0.929	0.506
$\Delta p/p$ compared with design orbit			1%
$\Delta R/R$			0.138%
$\eta = \frac{1}{\gamma^2} - \alpha_p$		0.366	0.310
$\gamma_t$		5.8	2.357
$\alpha_p$		0.030	0.18
$\beta$		0.778	0.715
$\gamma$		1.590	1.429
		One time injection	

## 4. Parameters of the B2B Transfer from ESR to CRYRING

TABLE XIII: Parameters related to the B2B transfer from the ESR to the CRYRING

		Proton/Antiproton	Heavy Ion
--	--	-------------------	-----------

	Unit	ESR Ext	CRYRING Inj	ESR Ext	CRYRING Inj
Design orbit	m	108.36	54.18	108.36	54.18
Ext orbit	m	108.36+0.15		108.36+0.15	
$C_{ESR} : C_{CRYRING}$		2.003		2.003	
Ext kinetic energy	MeV/u	30		4-10	
Inj kinetic energy	MeV/u		30		4-10
h		1	1	1	1
$f_{rf}$	MHz	0.685651	1.373200	0.254354-0.400885	0.509507-0.802879
$T_{rf}$	$\mu$ s	1.458	0.728	3.932-2.494	1.963-1.246
$f_{rev}$	MHz	0.685651	1.373200	0.254354-0.400885	0.509507-0.802879
$T_{rev}$	$\mu$ s	1.458	0.728	3.932-2.494	1.963-1.246
$\eta = \frac{1}{\gamma^2} - \alpha_p$		0.759		0.798-0.812	
$\gamma_t$		2.357		2.357	
$\alpha_p$		0.18		0.18	
$\beta$		0.248	0.248	0.092-0.145	0.092-0.145
$\gamma$		1.032	1.032	1.004-1.011	1.004-1.011
		One time injection		One time injection	

### 5. Parameters of the B2B Transfer from CR to HESR

TABLE XIV: Parameters related to the B2B transfer from the CR to the HESR

	Unit	Proton→ Antiproton		Heavy Ion→ RIB	
	Unit	CR Ext	HESR Inj	CR Ext	HESR Inj
Design orbit	m	221.45	575	221.45	575
$C_{HESR} : C_{CR}$		2.597		2.597	
Ext kinetic energy	GeV/u	3		0.74	
Inj kinetic energy	GeV/u		3		0.74
h		1	1	1	1
$f_{rf}$	MHz	1.316775	0.507131	1.124408	0.433043
$T_{rf}$	$\mu$ s	0.759	1.972	0.889	2.309
$f_{rev}$	MHz	1.316775	0.507131	1.124408	0.433043
$T_{rev}$	$\mu$ s	0.759	1.972	0.889	2.309
Max $\Delta p/p$		$\pm 3\%$		$\pm 1.5\%$	
$\eta = \frac{1}{\gamma^2} - \alpha_p$		-0.011		0.178	
$\gamma_t$		3.85		2.711	
$\alpha_p$		0.067			
$\beta$		0.972	0.972	0.830	0.830
$\gamma$		4.221	4.221	1.794	1.794
		100 times Injection per 10 seconds		100 times Injection per 10 seconds	

### 6. Parameters of the B2B Transfer from SIS100 to CR

TABLE XV: Parameters related to the B2B transfer from the SIS100 to the CR

		Proton→ Antiproton		Heavy Ion→ RIB	
	Unit	SIS100 Ext	CR Inj	SIS100 Ext	CR Inj
Design orbit	m	1083.6	221.45	1083.6	221.45
$C_{SIS100} : C_{CR}$		4.893		4.893	
Ext kinetic energy	GeV/u	28.8		1.5	
Inj kinetic energy	GeV/u		3		0.74
h		5(1 bunch)	1	2(1 bunch)	1
$f_{rf}$	MHz	1.383509	1.316778	0.511628	1.124408
$T_{rf}$	$\mu$ s	0.723	0.759	1.955	0.889
$f_{rev}$	MHz	0.276702	1.316778	0.255814	1.124408
$T_{rev}$	$\mu$ s	3.614	0.759	3.909	0.889
Max $\Delta p/p$		$\pm 3\%$		$\pm 1.5\%$	
$\beta$		0.9995	0.972	0.924	0.830
$\gamma$		31.918	4.221	2.610	1.794



		One time injection	One time injection
--	--	--------------------	--------------------